Inhibition and dynamics of a β-lactamase

Elings, W.

Chapter 2

Phosphate promotes the recovery of *Mycobacterium tuberculosis* β-lactamase from clavulanic acid inhibition

Based on the research article: Wouter Elings†, Raffaella Tassoni†, Steven A. van der Schoot, Wendy Luu, Josef P. Kynast, Lin Dai, Anneloes J. Blok, Monika Timmer, Bogdan I. Florea, Navraj S. Pannu, Marcellus Ubbink (2017). Phosphate promotes the recovery of Mycobacterium tuberculosis β-lactamase from clavulanic acid inhibition. Biochemistry 56, 6257-6267.*
The kinetics experiments described in this chapter were performed by Wendy Luu and Anneloes Blok, the simulations by Marcellus Ubbink, several of the inhibition experiments in cooperation with Steven van der Schoot and Anneloes Blok, the NMR titrations in cooperation with Josef Kynast and recording of the 3D NMR spectra by Marcellus Ubbink. Figure 2.7 was made by Qing Miao.

Abstract

The rise of multi- and even totally antibiotic resistant forms of *Mycobacterium tuberculosis* underlines the need for new antibiotics. The pathogen is resistant to β-lactam compounds due to its native serine β-lactamase, BlaC. This resistance can be circumvented by administration of a β-lactamase inhibitor. We studied the interaction between BlaC and the inhibitor clavulanic acid. Our data show hydrolysis of clavulanic acid and recovery of BlaC activity upon prolonged incubation. The rate of clavulanic acid hydrolysis is much higher in the presence of phosphate ions. A specific binding site for phosphate is identified in the active site pocket, both in the crystalline state and in solution. NMR spectroscopy experiments show that phosphate binds to this site with a dissociation constant of 30 mM in the free enzyme. We conclude that inhibition of BlaC by clavulanic acid is reversible and that phosphate ions can promote the hydrolysis of the inhibitor.

Introduction

With antibiotic effectiveness decreasing more rapidly than drug development can counter, the broad range, proven safety and ample availability of β-lactam antibiotics may provide new opportunities for treatment of *Mycobacterium tuberculosis* (Mtb) infection. The native resistance that this bacterium has to β-lactams can be circumvented by inhibition of

BlaC by β-lactam-like suicide substrates. The most common of these inhibitors is clavulanic acid and indeed, combinations of clavulanic acid with β-lactam antibiotics were found to be bactericidal against even extensively drug-resistant Mtb.[47,50,55,59]

Clavulanic acid inhibits BlaC in a substrate-like fashion, forming a covalent bond with the catalytic serine (Ser70 by standard Ambler notation[17]). Generally, in class A β-lactamases, it can then form a variety of covalently bound fragmentation products in the active site, leaving the enzyme either transiently or irreversibly inactivated.[38] For BlaC, several of these products have been found.[18,74,130] Formation of these inactive forms was initially reported to be irreversible in BlaC,[18] but slow recovery of activity was reported thereafter.[41]

A crystal structure of a covalent adduct formed between BlaC and clavulanic acid was published by Tremblay *et al.*[130] Interestingly, this structure models a well resolved phosphate ion in the carboxylate binding site, immediately adjacent to the bond between enzyme and adduct. At the same position, a phosphate ion can also be found in several other BlaC crystal structures.[29,44,131–133] In fact, in 26 of the 29 BlaC crystal structures that have been published to date, this position was found to be occupied by either a phosphate ion or a carboxylate group of the ligand that was used for co-crystallization. Additionally, Xu *et al.* notice that in their structure of BlaC with avibactam (PDB: 4DF6), the sulfate group of the inhibitor occupies this position.[41] The authors of these studies either do not mention the active site phosphate they model, or assume that it is an artefact of the high phosphate concentration under crystallization conditions. We investigated the role of the phosphate ion and demonstrate that it affects the rate of recovery from clavulanic acid inhibition. We also show that a phosphate ion binds to the enzyme in solution in the active site.

Results

BlaC is normally produced by *M. tuberculosis* with an N-terminal Tat-type signal peptide that is used to locate BlaC as a lipoprotein on the outside of the cell membrane.[24,134,135] To obtain soluble protein for *in vitro* experiments, a BlaC gene encoding only the soluble beta-lactamase domain supplemented with a C-terminal 6xHistidine purification tag was expressed in *E. coli*. The protein was isolated and purified using immobilized metal affinity chromatography and subsequent size exclusion chromatography to yield *ca.* 30 mg BlaC per liter of culture medium.

The Michaelis-Menten kinetic parameters of nitrocefin hydrolysis by BlaC were determined in buffers with and without phosphate (Table 2.1, Figure S2.1). The measured Michaelis constant K_m is higher in phosphate buffer than in the other tested buffers. This effect appears to be somewhat compensated by a higher catalytic efficiency at pH 6.

Table 2.1. Buffer dependence of nitrocefin hydrolysis by BlaC. [a]

Buffer	k_{cat} (s^{-1})	K_m (μM)	k_{cat}/K_m ($\cdot 10^5$ $M^{-1}s^{-1}$)
NaPi pH 6.0	107 ± 6	147 ± 14	7.3 ± 0.4
NaPi pH 7.0	64 ± 6	153 ± 23	4.2 ± 0.2
MES pH 6.0	69 ± 1	38 ± 7	18 ± 3
BIS-TRIS pH 6.0	83 ± 3	61 ± 7	14 ± 1

[a] Buffer concentrations were each 100 mM. Errors represent the standard deviation over triplicate measurements.

These results are in agreement with previously published kinetic values for BlaC nitrocefin hydrolysis, which have k_{cat}/K_m in the range of 4–18 $\cdot 10^5$ $M^{-1}s^{-1}$.[18,22,29,74] Similar to most of these studies, further experiments have been performed at pH 6.4, which is the optimum pH for BlaC. The work in this study was performed on BlaC with a C-terminal His-tag (Figure S2.2). To ensure that the tag has no effect on the activity, we also prepared BlaC with a cleavable N-terminal His-tag (Figure S2.3). The kinetic parameters of nitrocefin hydrolysis by BlaC without His-tag were then compared to those of the His-tagged BlaC used in this study and were found to be the same, at k_{cat}/K_m of 10 $\cdot 10^5$ $M^{-1}s^{-1}$ and 11 $\cdot 10^5$ $M^{-1}s^{-1}$, respectively, in 100 mM MES pH 6.4 (Table S2.1).

Next, BlaC inhibition by clavulanic acid was studied. For this, Hugonnet and Blanchard proposed a reactivation model, equation (2.1), including fast binding of the inhibitor *I* to the enzyme *E* to form the *EI* complex, followed by slower conversion to the long-lived *EI** complex.[18]

$$E + I \underset{k_{-1}}{\overset{k_1}{\rightleftharpoons}} EI \underset{k_{-2}}{\overset{k_2}{\rightleftharpoons}} EI^* \qquad (2.1)$$

Using this approach, they determined the affinity constant for BlaC clavulanic acid inhibition ($K_i = k_{-1}/k_1$) to be 12.1 μM, the inactivation rate k_2 2.7 s^{-1} and reactivation rate k_{-2} indistinguishable from zero. This led to the conclusion that clavulanic acid inhibition of BlaC is irreversible. To study the variation of inhibition kinetics with buffer conditions, we used the reactivation model with the adjustment proposed by Xu *et al.*[41] (2.2), in which conversion of covalently bound clavulanic acid *EI** into a product *P* is allowed with a rate constant k_3, rather than reversal of the covalent linkage to the active site serine residue with a rate constant k_{-2}.

$$E + I \underset{k_{-1}}{\overset{k_1}{\rightleftharpoons}} EI \overset{k_2}{\rightarrow} EI^* \overset{k_3}{\rightarrow} E + P \qquad (2.2)$$

As clavulanic acid acts as a slow-onset inhibitor for BlaC, reaction rates can be estimated from the rate at which enzymatic activity decreases upon administration of the inhibitor.

The resulting inhibition curves are plotted in Figure 2.1 for phosphate buffer and Figure S2.4 for MES buffer. These data were fitted to equation (2.3) to obtain the apparent first-order rate constants (k_{iso}) of inhibition for each clavulanic acid concentration, which were then fitted to equation (2.4) to estimate the rate constants of inhibition (Table 2.2). The mathematical description of k_{iso} given in equation (2.4) is the same for the reactivation model of Hugonnet and Blanchard[18] and the conversion model of Xu *et al.*,[41] except k_{-2} is replaced by k_3. However, the latter model predicts that in time clavulanic acid will be degraded and BlaC will regain activity, whereas the former model predicts that an equilibrium is reached and BlaC will remain inhibited. The latter model applies, as is discussed below.

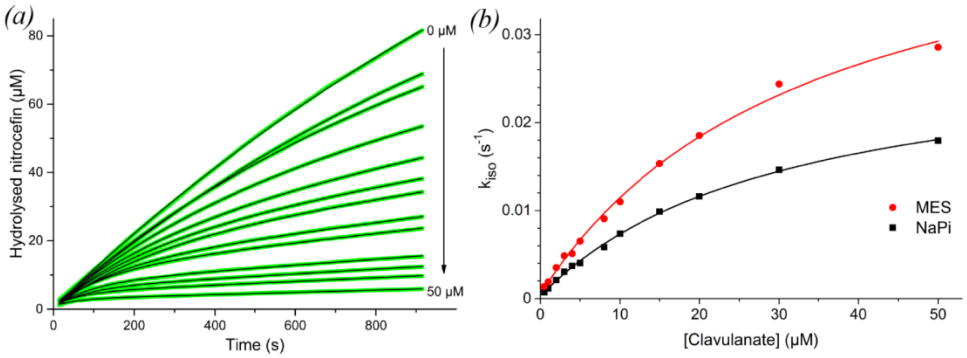

Figure 2.1: *(a)* Inhibition curves of BlaC nitrocefin hydrolysis with increasing concentrations of clavulanic acid in 100 mM NaPi, pH 6.4. Green lines represent experimental data, black lines are fits using equation (2.3). *(b)* Plot of k_{iso} values obtained from the fit of each inhibition curve against the respective clavulanic acid concentration, for MES (red circles) as well as NaPi (black squares) buffer. The solid lines represent the fits to equation (2.4).

Table 2.2. Rate constants of BlaC inhibition with clavulanic acid. [a,b]

	Approach	K_i (µM)	k_2 (10^{-2} s^{-1})	k_3 (10^{-4} s^{-1})
NaPi pH 6.4	fit to eq. (2.3) & (2.4)	32 ± 2	2.9 ± 0.1	4 ± 1
	Simulation	20	4.5	18
MES pH 6.4	fit to eq. (2.3) & (2.4)	35 ± 4	4.9 ± 0.3	6 ± 3
	simulation	20	4.5	0.25

[a] Parameters may be correlated, values should therefore be interpreted as indicative.
[b] Errors represent the standard errors of the fit.

The fits of the inhibition curves follow the data remarkably accurately. However, variation of the parameters of the fit shows that they are correlated and other combinations can be obtained that yield equally accurate fits. To evaluate the quality of the data and the values of the parameters, the data were also simulated by solving the differential equations underlying the kinetic model numerically using GNU Octave software. Good simulations

(Figure S2.5) were obtained with the values listed in Table 2.2. All parameters are listed in Table S2.2. These simulations show that curves contain small errors in the offset and in the shape due to measuring artefacts, which are faithfully fitted in the first approach. This suggests that the parameters derived from the k_{iso} curves may not be very accurate, due to overfitting. In short, the method relies on too many parameters to yield quantitative results. It is qualitatively clear, however, that the slopes of the last parts of the curves (i.e. the v_s values in eq. 1, or the k_3 values in the simulations) are close to zero in the presence of high concentrations of clavulanic acid in MES buffer, but not in phosphate buffer. This finding implies that hydrolysis of clavulanic acid by BlaC is much faster in phosphate buffer.

To test the rate of clavulanic acid hydrolysis in a more direct manner, the recovery of activity after inhibition was assayed. BlaC was incubated with a 5-fold excess of clavulanic acid and samples were taken over time and tested for nitrocefin hydrolase activity. Activity was observed to return after a characteristic delay time, reproducible over different batches of enzyme and inhibitor but dependent on reaction conditions (Figure 2.2, Table 2.3). At 20 µM BlaC with 100 µM clavulanic acid in 100 mM MES pH 6.4, Hugonnet and Blanchard[18] observed no return of activity within 12 hours. We find that recovery occurs after *ca.* 14 hours. Moreover, recovery was *ca*. 22 times faster in phosphate buffer than in MES buffer under the same conditions. Addition of sulfate to the MES buffer resulted in *ca*. 7 times faster recovery, whereas addition of acetate slowed the recovery down ca. 2.6 times. Turn-over rates were defined as the number of clavulanic acid molecules inactivated per enzyme molecule per second and were derived from the 50% recovery times. The turn-over rates, listed in Table 2.3, are close to those derived from the simulations of the inhibition data (k_3 values in Table 2.2). Interestingly, at a high concentration of BlaC (300 µM), in 100 mM MES, recovery was found to be about two times faster than that at 100 or 20 µM, with the same clavulanic acid-to-enzyme ratio of 5:1. To investigate whether this was due to an allosteric effect of clavulanic acid at high concentration, the recovery time was measured for solutions with 100 µM BlaC and increasing concentrations of clavulanic acid, from 100 to 1500 µM. The total recovery time increased linearly with the concentration of clavulanic acid (Figure S2.6 and Figure S2.7), indicating that the turn-over rate of BlaC was constant. Thus, it is concluded that the increase in turn-over rate only occurs at very high BlaC concentration (300 µM), perhaps due to a weak protein-protein interaction. However, this effect is unlikely to be relevant under physiological conditions and was not investigated further. No significant concentration dependence of the turn-over rate was seen in phosphate buffer.

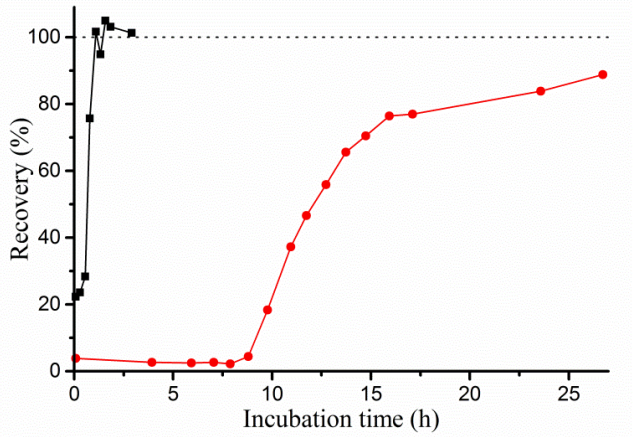

Figure 2.2. Example curves of BlaC recovery from clavulanic acid inhibition. 20 µM BlaC was incubated with 100 µM clavulanic acid in 100 mM NaPi (black squares) or MES (red circles) buffer, pH 6.4. Samples were taken at various time points, diluted to 2.0 nM BlaC and tested for hydrolase activity using 100 µM nitrocefin. BlaC and clavulanic acid separately were each stable throughout the experiments (data not shown). The activity of inhibited enzyme is non-zero due to recovery taking place in the time between initial dilution and activity measurement of the samples (~ 5 min).

Table 2.3. Rates of BlaC activity recovery from clavulanic acid inhibition. [a]

Buffer	[BlaC] (µM)	[Clavulanic acid] (µM)	Ratio	50% recovery time (h)	Turnover rate ($\cdot 10^{-4}$ s^{-1})
MES [b]	20	100	1 : 5	14 ± 1	1.03 ± 0.07
MES [c]	100	100	1 : 1	1.8 ± 0.8	1.5 ± 0.7
MES [c]	100	300	1 : 3	7 ± 0.8	1.2 ± 0.1
MES [c]	100	500	1 : 5	13.8 ± 0.8	1.01 ± 0.06
MES [c]	100	1000	1 : 10	28 ± 0.8	0.99 ± 0.03
MES [c]	100	1500	1 : 15	43.5 ± 1	0.96 ± 0.02
MES [d]	300	1500	1 : 5	6.0 ± 0.6	2.3 ± 0.2
MES + 100 mM acetic acid [c]	100	500	1 : 5	36 ± 3	0.38 ± 0.03
MES + 100 mM Na_2SO_4 [c]	100	500	1 : 5	2.0 ± 0.5	7 ± 2
NaPi [b]	20	100	1 : 5	0.63 ± 0.06	22 ± 2
NaPi [d]	300	1500	1 : 5	0.82 ± 0.01	16.8 ± 0.3

[a] Buffers were all 100 mM, pH 6.4.
[b] Errors are the standard deviations over 4 replicates.
[c] Errors are the estimated error in half-time determination of single experiments.
[d] Errors are the standard deviations over 2 replicates.

To gain insight in the inhibition intermediates that arise, samples were analyzed using whole-protein mass spectrometry (Figure 2.3). Before inhibition, the enzyme was present in three forms, with the theoretical mass of BlaC as the main species and minor additional

species with relative masses of *ca*. –19 and –35 present. It is unclear how these latter two species differ from the native enzyme or whether this is an artefact of the sample treatment and MS analysis. Upon inhibition with clavulanic acid, these peaks diminish and species of *ca.* +35, +51 and +70 appear instead. The consistent relative intensities and mass differences of +70 relative to the three unbound peaks (–19 + 70 = +51; –35 + 70 = +35) suggest that these peaks represent a single inhibition intermediate. This is likely the propionaldehyde ester that was previously reported upon inhibition of BlaC with clavulanic acid.[18,130] Several other peaks also appear, including *ca*. +86, +136 and +154 species. The *ca.* +86 intermediate has not been observed for inhibition of BlaC with clavulanic acid before, but may correspond to the hydrated propionaldehyde (+88) that was observed upon clavulanic acid inhibition of related β-lactamases.[38] The *ca.* +154 and +136 adducts were previously observed as BlaC clavulanic acid intermediates and these were proposed to represent a decarboxylated *trans*-enamine adduct and its dehydrated variant, respectively.[18,130] Interestingly, although the observed masses are similar to previous results, their relative intensities are not. The BlaC +154 enamine was previously reported as the major dead-end product. However, we observe mainly the +70 aldehyde adduct that was previously reported as minor and decreasing over time. We observed only minor changes in relative intensities upon prolonged incubation, even upon incubating at higher clavulanic acid : BlaC ratios to achieve higher turn-over numbers (Figure 2.3, right). Instead, concurrent with the return of activity, all species were observed to diminish and the original masses returned. Remaining peaks could indicate either irreversible inhibition products or incomplete recovery, but these peaks were relatively low in intensity. Furthermore, although the time required for enzyme recovery was influenced greatly by the presence or absence of phosphate, no effect on the type of intermediates was observed (Figure S2.8).

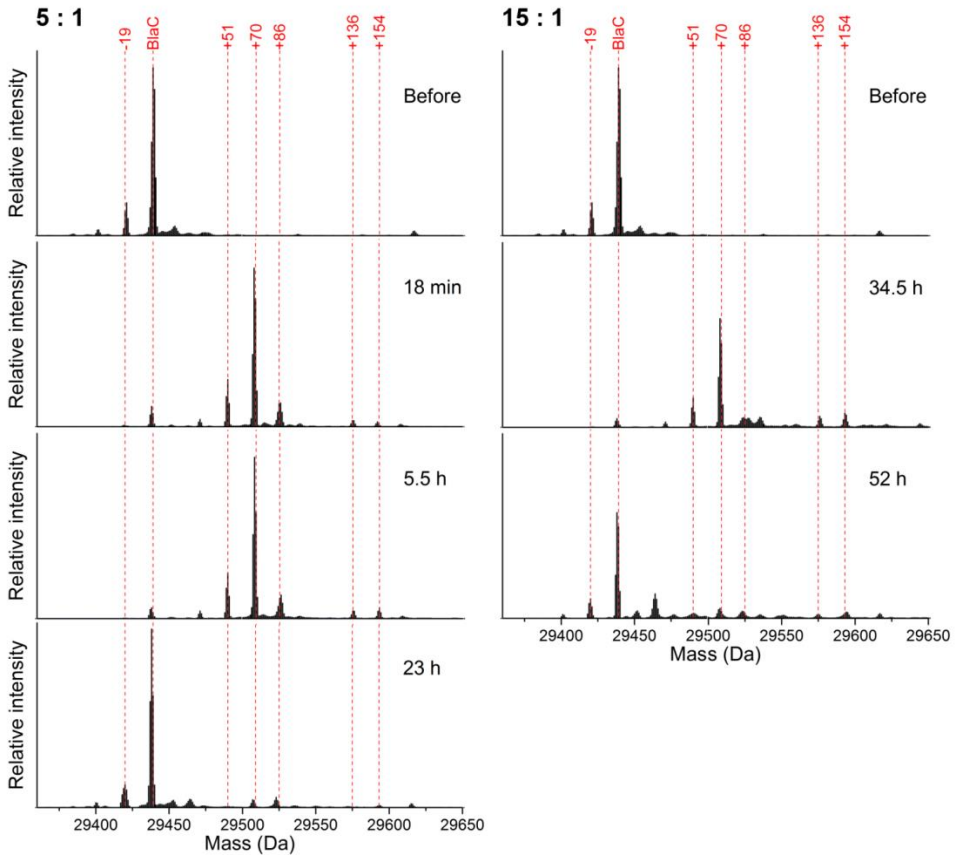

Figure 2.3. Charge-deconvoluted mass spectra of BlaC before and during incubation at 100 µM BlaC with 500 (left) or 1500 (right) µM clavulanic acid in 100 mM MES, pH 6.4. Upon inhibition with clavulanic acid, the main species contain covalently bound adducts. After prolonged incubation, the enzyme returns to its free form. The lowest spectra on either side correspond to recovered enzyme activity in the samples. The MS data were obtained using a Waters Synapt mass spectrometer. Each spectrum was normalized to the total signal intensity.

The interaction between phosphate and BlaC was further corroborated by Raffaella Tassoni,[136] who showed specific binding of phosphate in the carboxylate binding site in a 1.19 Å resolution crystal structure (Figure 2.4a). It is available in the Protein Data Bank (PDB) as entry 5NJ2. She furthermore showed that acetate can also bind to this site (Figure 2.4b), this crystal structure is available as PDB entry 5OYO.

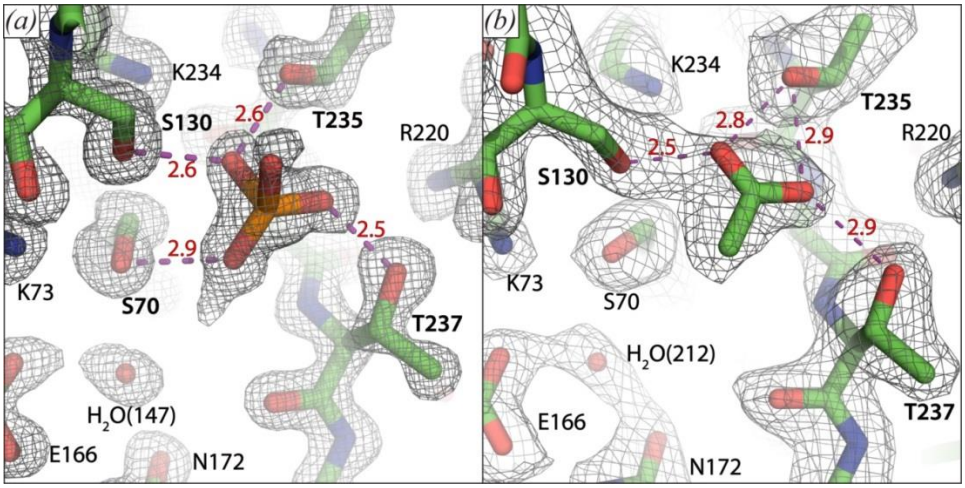

Figure 2.4. Close-up on the carboxylate binding sites of BlaC crystal structures 5NJ2, chain A *(a)* and 5OYO chain B *(b)*. Several catalytically important residues and a conserved active site water molecule are indicated. Distances (in Å) of proposed hydrogen bridges (purple dashed lines) involving the phosphate group and acetate are indicated in red. The mesh shows the $2F_o - F_c$ electron density map contoured at 1.5 σ *(a)* or 1.0 σ *(b)*.

To establish whether BlaC also interacts with phosphate in the solution state, we used nuclear magnetic resonance spectroscopy (NMR). As NMR studies of BlaC have not been reported before, a set of standard 3D NMR spectra was recorded to perform sequential backbone assignment. With these, 98% of the BlaC backbone H-N moieties were assigned to a resonance peak in the corresponding ^{1}H-^{15}N heteronuclear single quantum coherence (HSQC) spectrum (Figure S2.9). Interestingly, the four residues at hydrogen-bonding distance from the active site phosphate (Figure 2.4a) were the only non-proline, non-terminal residues whose backbone resonances could not be identified in the spectra, suggesting that their amide nuclei are in intermediate exchange, causing line broadening of the NMR resonances. The assignment data are available at the Biological Magnetic Resonance Bank under ID 27067.

We then acquired 2D HSQC spectra of BlaC at phosphate concentrations varying from 0 – 250 mM (Figure S2.10). Multiple resonances were found to shift position, indicating that the corresponding residues experience fast exchange between different chemical environments. At low phosphate concentrations only a few peaks were affected, showing large chemical shift perturbations (CSPs, defined as $|\Delta\delta(^{1}H)| + |0.2*\Delta\delta(^{15}N)|$), whereas CSPs for many resonances were observed at higher phosphate concentrations (>50 mM). When mapped on the protein structure, it becomes apparent that the large CSPs arise for nuclei close to the position in the active site where phosphate is present in the crystal structure (Figure 2.5, left). The smaller CSPs that appear at high phosphate concentration represent much weaker phosphate binding at other sites. The data allowed us to determine the binding affinity in solution. By analyzing the magnitude of active-site CSPs

as a function of the phosphate-BlaC ratio, a binding affinity (K_D) of 27 ± 11 mM was found for phosphate binding to BlaC (Figure 2.5, right). A separate titration with sodium chloride (Figure S2.11) did not result in any CSPs with the magnitude, co-localization or affinity of those found for phosphate, confirming that the observed effects are caused by a specific interaction.

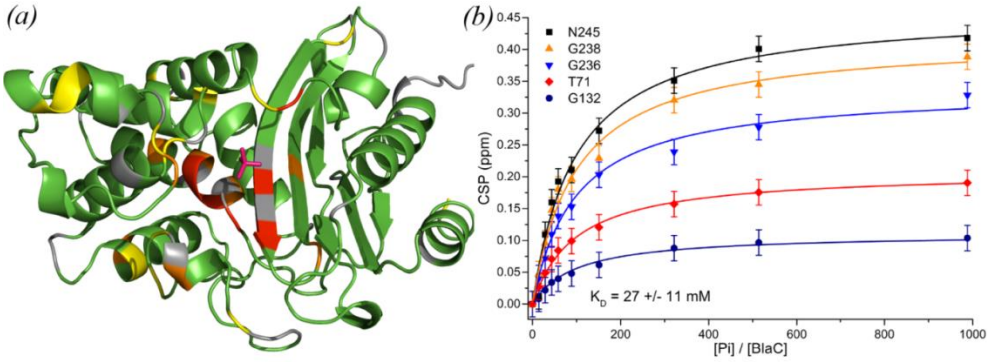

Figure 2.5. BlaC-phosphate interaction. *(a)* Crystal structure 5NJ2 is shown with residues that are affected by phosphate binding in solution highlighted. Residues of which the amide backbone experienced CSPs over 0.075, 0.10 and 0.15 ppm are displayed in yellow, orange and red, respectively, whereas the ones for which no data were available are displayed in grey and those with no or small CSPs are colored green. The phosphate as observed in the crystal structure is indicated in magenta. *(b)* Binding curves. The plot shows the CSPs upon phosphate titration for five selected amide resonances plotted against the ratio of the phosphate and BlaC concentrations. Data points are shown with an estimated peak picking error of ±0.02 ppm, error in K_D is the standard deviation over duplicate titrations.

NMR spectroscopy was also used to study the BlaC clavulanic acid interaction. Upon addition of a fivefold excess of clavulanic acid, several peaks disappeared and new peaks appeared nearby. Unsurprisingly, the corresponding nuclei were located in the active site (Figure 2.6a). Upon prolonged incubation, the peaks of the unbound state reappeared and the peaks of the bound state disappeared. This observation indicates that the free and bound forms are not in exchange on the chemical shift time scale (exchange rate << 100 s^{-1}), in line with the expected formation of a covalent intermediate. The recovery times of free BlaC after incubation with fivefold excess of clavulanic acid based on the NMR peak intensities (Figure 2.6b) were in agreement with the kinetics and MS data (Table 2.3), including data taken directly on the NMR samples.

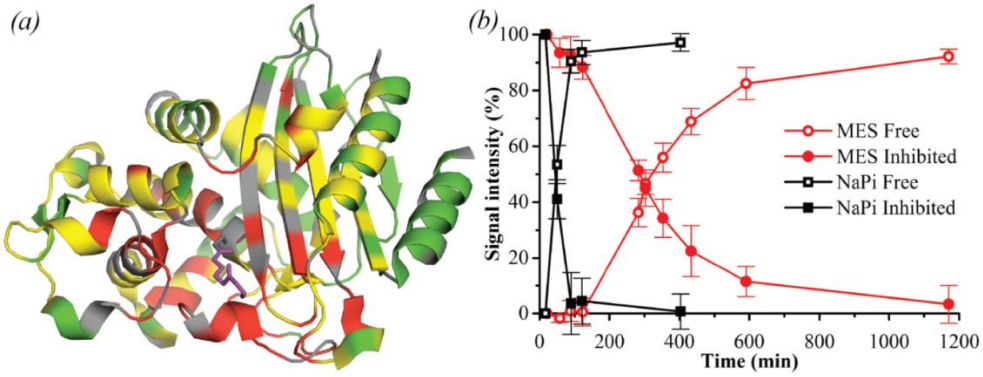

Figure 2.6. Effect of clavulanic acid on BlaC as measured by NMR. *(a)* Crystal structure 3CG5[130], highlighting residues of which NMR resonances are affected by addition of clavulanic acid. Residues of which the amide backbone resonance experienced CSPs over 0.01 ppm and over 0.05 ppm are displayed in yellow and red, respectively, while the ones for which no data were available are displayed in grey and the remaining residues in green. The bound reacted adduct of clavulanic acid as was observed by Tremblay *et. al.*[130] is shown in purple sticks. *(b)* Effect of clavulanic acid on BlaC over time, in 100 mM MES (red circles) and NaPi (black squares) buffer, pH 6.4. Data points show average and standard deviation of relative signal intensities from the native (open symbols) and inhibited (filled symbols) resonances of residues Cys69, Ala74, Asp131, Ala146 and Tyr241.

Discussion

In this work, BlaC and its interaction with clavulanic acid were further characterized *in vitro*. The Michaelis-Menten kinetic values found for nitrocefin hydrolysis are largely consistent with previous observations, although an elevation of the Michaelis constant was observed in the presence of phosphate. This may point toward competition between phosphate and substrate for occupation of the carboxylate binding site. This explanation would lend further credence to the suggestion by Kurz *et al.*[42] that the same competition may explain their observation of an oddly placed carbonyl moiety in co-crystallization of BlaC with a boronic acid transition state inhibitor. To determine the reaction rates with clavulanic acid, the model proposed by Xu *et al.*[41] was used (eq. 7). It should be noted that clavulanic acid chemistry may be more complicated than this model suggests, as various inhibition intermediates have been reported[18,130] and observed in this study. Presumably, different inhibition intermediates will have different rates of formation and decomposition.

The approach of fitting inhibition curves to initial and final velocities (v_i and v_s) and an exponential decay constant (k_{iso}) that describes the time to reach a steady state inhibition level, has been used frequently. Our simulations of the curves suggest that the method may lead to overfitting of the parameters and should be used with caution. In particular the rate constant for hydrolysis of the covalent intermediate (k_3) is poorly defined. This

rate is very low and its value depends heavily on the fits of the lowest inhibitor concentrations. The parameters of clavulanic acid inhibition onset that we found are in reasonable agreement with the K_i = 12.1 µM and k_2 = 2.7 s^{-1} found by Hugonnet and Blanchard,[18] who used the same approach described here except for their assumption that the covalent intermediate is not hydrolyzed (k_3 = 0). We found that BlaC slowly converts clavulanic acid to regain activity, consistent with the observations of Xu *et al.*[41] The return to the native active form of the protein was demonstrated by activity assays, NMR spectroscopy and mass spectrometry.

The main covalent intermediate of inhibition was observed to harbor a *ca.* +70 mass compared to the non-inhibited protein, corresponding to the adducts observed by Hugonnet and Blanchard[18] upon inhibition with each of the inhibitors clavulanic acid, sulbactam and tazobactam and proposed by them and others to be a hydrolysable aldehyde adduct. However, the +136 and +154 clavulanic acid enamine adducts observed as main, dead-end, reaction products by Hugonnet and Blanchard[18] as well as Xu *et al.*[130] were observed in only minor quantities in our analysis. We demonstrate that the rate of recovery is highly dependent on reaction conditions. Phosphate ions enhance the rate, yet the composition of the inhibition intermediates is not affected. This indicates that phosphate promotes the release of covalently bound clavulanic acid adducts from the active site and does not change the direction of the initial chemistry. NMR experiments support phosphate ion binding in the active site and show that the dissociation constant is 3 x 10^{-2} M. This affinity requires that at crystallization conditions of 2 M phosphate, the site should be fully occupied. This is consistent with the observations published so far. We note that structure 2GDN is the only BlaC structure that was modelled with an empty carboxylate binding site, despite a high phosphate concentration in the crystallization buffer, but the data do show density that suggests the presence of a phosphate ion there. The high resolution structure by Raffaella Tassoni shows that the phosphate is in hydrogen bond distance to several important active site residues and may be protonated at the phosphate oxygen close to Ser70.

To formulate a hypothesis about the role of phosphate in promoting hydrolysis, we examined the structure of BlaC covalently bound to a cleavage product of clavulanic acid (PDB entry 3CG5,[130] Figure 2.7). It should be noted that the intermediate in structure 3CG5 is not the dominant species observed in our work, of +70 Da, but the ester bond to Ser70 is likely to be in a similar place in all intermediates. In this structure, a phosphate (PO_4 309) is present in the same location as in the structure of substrate free BlaC, although it is slightly displaced by the presence of the adduct. Most likely, the carboxylate binding site is also involved in the initial interaction between BlaC and the carboxy group of clavulanic acid, but it becomes available upon decarboxylation of the acyclic adduct. This reaction occurs rapidly and appears to create enough space to allow for diffusion of phosphate into the carboxylate binding site. In the second step of the reaction, a nucleophilic attack on

the carbon (atom CAG in structure 3CG5) of the adduct forming the ester bond with Ser70 occurs, the bond between Ser70 and the adduct is broken, and Ser130 O_γ is reprotonated. The nucleophilic attack can be executed by water 441, located at 3.1 Å underneath the ester bond plane and hydrogen bonded to Glu166. This is the standard mechanism of β-lactamase hydrolysis. However, O_3 of the phosphate is located also at 3.1 Å of the CAG carbon and right above the ester bond plane. So, alternatively, the phosphate could carry out the nucleophilic attack. After release from the enzyme, the phospho-adduct would probably be rapidly hydrolyzed.

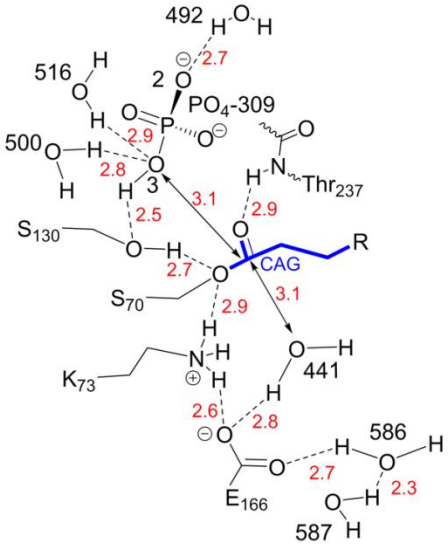

Figure 2.7. Schematic representation of catalytically important groups and their hydrogen-bonding network, as present in structure 3CG5[130] of BlaC with a clavulanic acid cleavage product (indicated in blue) covalently bound to Ser70. Distances (in Å) between heavy atoms involved in potential H-bonds are shown in red. Residues are numbered according to the Ambler consensus,[17] other numbers represent the internal numbering of the published structure.

An alternative role of the phosphate could be in reprotonation of the Ser70 O_γ. The distance between the phosphate oxygen O_3 and the Ser70 O_γ is larger (3.5 Å) than in the substrate free structure (2.9 Å, Figure 2.4a) but it is close to the O_γ of Ser130 (2.5 Å). If the nucleophilic attack is performed by the water, a proton would be donated to Glu166. This glutamate is hydrogen bonded to the amine of Lys73, which also forms an H-bond with Ser70 O_γ, allowing for proton transfer to Ser. Alternatively, the Ser70 O_γ could be reprotonated by accepting the proton from Ser130 (O-O distance 2.7 Å), which in its turn accepts a proton from O_3 of the phosphate (Figure 2.7). The phosphate is in contact with waters on the protein surface (HOH 492, 500 and 516). In this case, Glu166 could release its proton by a flip of the carboxy group and donation of a proton to the nearby water chain (HOH 586 and HOH 587).

Our data show that sulfate can also accelerate hydrolysis of clavulanic acid, albeit less than phosphate. It can be expected that the sulfate ion is fully deprotonated at pH 6.4, so it could not act as a hydrogen donor to Ser130. However, it could act as a nucleophile to attack carbon CAG. One BlaC structure, PDB 3ZHH,[30] shows sulfate bound in the carboxylate binding site, in a similar location as the phosphate. The limited resolution does not allow for a detailed analysis. Raffaella Tassoni also solved the structure of BlaC with excess acetate. Acetate in MES buffer has a negative effect on the hydrolysis rate as compared to MES buffer only. This observation cannot be readily explained, but the data show acetate binding in the carboxylate binding site. It forms a hydrogen bond with Ser130, so could act as a hydrogen bond donor. In an overlay of 3CG5 and our structure 5OYO, it can be seen that the closest oxygen of the acetate is at 4.2 Å of the CAG carbon, making a nucleophilic attack unlikely. We cannot exclude that MES buffer (2-(N-morpholino)ethanesulfonic acid) can bind to the carboxylate binding site as well, via its sulfonate group, having a weak positive effect on the rate of hydrolysis. Acetate could be competing with MES, leading to a reduction of the rate. These considerations point to a role of phosphate and sulfate as alternative nucleophiles. We emphasize, however, that the proposed mechanisms are speculative. Further research is required to understand the influence of anions on the hydrolysis rate of clavulanic acid. Clearly, the binding site is promiscuous and various ions have quite different effects on hydrolysis.

It is worthwhile to consider whether the effect we observe is specific for BlaC, or if it may signify a more general mechanism in class A β-lactamases. Indeed, related proteins such as TEM-1, SHV-1 and CTX-M-1 have very similar carboxylate binding sites. However, most of these enzymes harbor an Ala at position 237, where BlaC has a Thr, which contributes a hydrogen bond to the binding of phosphate (Figure 2.4a). Indeed, although phosphates and sulfates have been observed to occupy analogous positions in at least TEM-1,[32] CTX-M-9[137] and L2,[138] many x-ray structures of these enzymes with empty carboxylate binding site have also been reported (e.g. structure 3CMZ[139] of TEM-1 and structure 1SHV[33] of SHV-1). These observations suggest that the affinities between these proteins and phosphate-like groups may be lower than in the case of BlaC. We therefore expect any effect of phosphate in related enzymes to be less significant. Whether the role of phosphate and other anions in the breakdown of clavulanic acid by BlaC is relevant under physiological conditions is unclear. *M. tuberculosis* is known to prevent maturation of lysosomes by blocking phagolysosomal fusion and has been shown to live at slightly acidic pH.[140] The experiments reported here have been conducted at pH 6.4, which is the optimal pH of BlaC and can thus be expected to be physiologically relevant. The concentration of phosphate ions in *M. tuberculosis* within macrophages is unknown. Total prokaryotic and eukaryotic intracellular phosphate ion concentrations, however, are in the 1 – 10 mM range.[141] Additionally, sulfate ions were observed to have a similar effect and it cannot be excluded that other compounds, such as ATP, can also interact with BlaC. Thus,

it is reasonable to expect that a substantial fraction of BlaC molecules binds a phosphate-like group specifically in the active site.

Materials And Methods

Materials

NMR analysis indicated that the nitrocefin purchased from BioVision Inc. and Oxoid Limited was significantly purer than that from Cayman Chemicals. The BioVision nitrocefin was used in this study. Several values have been reported for the change in extinction coefficient upon hydrolysis of nitrocefin (e.g. [22,74]). To determine this value independently, a stock solution containing 5.0 mg of nitrocefin was diluted to a range of seven concentrations from 10-75 µM in 100 mM sodium phosphate buffer, pH 6.4. The A_{486} values before and after complete hydrolysis by 20 minutes incubation with 5 nM BlaC were determined. The slope of a linear fit of ΔA_{486} against nitrocefin concentration yielded $\Delta\varepsilon_{486}$. The procedure was performed in duplicate, yielding a $\Delta\varepsilon_{486}$ of 17 ± 1 mM^{-1} cm^{-1}. Clavulanic acid powder is hygroscopic, so its concentration was determined by the absorbance at 256 nm in NaOH. The extinction coefficient was determined by quantitative NMR versus a standard of trimethylsilylpropanoic acid. For ChemCruz and Matrix clavulanic acid, which are sold in a cellulose matrix, we found identical UV-Vis spectra, yielding an absorbance at 256 nm of 20.0 +/- 0.1 mM^{-1} cm^{-1}. For TRC clavulanic acid, which is a pure powder, the UV-vis spectrum is clearly different and the NMR spectrum shows impurities. The extinction coefficient at 256 nm is 18.7 mM^{-1} cm^{-1}.

Production and purification of BlaC

The *blaC* gene, lacking codons for the N-terminal 42 amino acids that constitute the signal peptide and with the addition of a C-terminal histidine tag (Uniprot P9WKD3 modified as specified in Figure S2.2), was expressed using a host optimized sequence (ThermoFisher Scientific), cloned in the pET28a vector in *Escherichia coli* BL21 (DE3) pLysS cells. The cells were cultured in LB medium at 310 K until the optical density at 600 nm reached 0.6, at which point expression was induced with 1 mM IPTG and incubation continued at 289 K overnight. For the production of isotope labelled proteins for NMR experiments, LB medium was replaced with M9 medium (Table S2.3) containing ^{15}N ammonium chloride (0.3 g/L) as the sole nitrogen source and, where necessary, ^{13}C D-glucose (4.0 g/L) and $^{2}H_2O$ (99.8%) as carbon and hydrogen source, respectively. Cells were harvested by centrifugation and lysed with a French press in a buffer of 50 mM Tris-HCl pH 7.5 containing 500 mM NaCl. After centrifugation, the soluble fraction was loaded on a HisTrap Nickel column (GE Healthcare) and eluted with a gradient of 0 - 250 mM imidazole in the same buffer. A Superose 12 10/300 GL size exclusion chromatography column (GE Healthcare) was used for further purification. Protein concentration and buffer exchange were performed using 10 kDa cut-off Amicon Ultra centrifugal filter units (Merck Millipore

Ltd). Protein purity was determined by SDS-PAGE (Figure S2.12) and concentrations were determined by the absorption at 280 nm, using the theoretical extinction coefficient ε_{280} = 29910 M^{-1} cm^{-1}.[142] BlaC with a TEV-cleavable His-tag (sequence specified in Figure S2.3) was produced in the same way, with additional cleavage of the purified protein by His-tagged TEV protease. Subsequent re-purification using another HisTrap Nickel column (GE Healthcare) yielded pure, His-tag-less BlaC in the flowthrough. Cleavage was confirmed by MS using a Waters Synapt spectrometer yielding a mass of 28637 ±1 Da, corresponding with 100% cleavage and 96% efficiency of the applied ^{15}N-labelling. No other protein forms, such as the non-cleaved construct (expected mass 31770 Da at 96% ^{15}N labelling), were detected in the final sample.

Kinetics

All kinetic measurements were performed by measuring hydrolysis of the chromogenic reporter substrate nitrocefin at 486 nm, using a Perkin-Elmer Lambda 800 UV-VIS spectrometer thermostated at 298 K. To determine Michaelis-Menten kinetic constants, initial nitrocefin hydrolysis rates by 5.4 nM BlaC were measured in 100 mM of the specified buffers, in triplicate. OriginPro 9.1 was used to fit standard Michaelis-Menten curves to these data. Reported are, for each condition, the average and standard deviation of the three independent fits.

The apparent first-order rate constants of inhibition (k_{iso}) were obtained by fitting the hydrolysis of 125 µM nitrocefin by 2 nM BlaC in the presence of various concentrations of clavulanic acid against equation (2.3).[18]

$$[P] = v_s\, t + \frac{v_i - v_s}{k_{iso}} [1 - e^{-k_{iso}\, t}] \qquad (2.3)$$

[*P*] Is the concentration of product in µM, v_s and v_i are the final and initial reaction velocities in the presence of inhibitor in µM s^{-1}, respectively, t is time in s and k_{iso} is the apparent first-order rate constant for the progression from v_i to v_s in s^{-1}. Subsequently, the rate constants of inhibition were obtained by fitting these data against Equation (2.4),[41] in which k_3 and k_2 are the rate constants for step 3 and 2 in the conversion model (2.2) (see Results section), respectively, while K_i is the ratio k_{-1} / k_1 in that model.

$$k_{iso} = k_3 + \frac{k_2\,[I]}{K_i + [I]} \qquad (2.4)$$

The data were also simulated using GNU Octave 3.2.4 and numerical simulations of the differential equations derived from the following model.

$$N + E \underset{k_{-a}}{\overset{k_a}{\rightleftharpoons}} NE \overset{k_b}{\rightarrow} I_1 \overset{k_c}{\rightarrow} P_1 + E \qquad (2.5)$$

$$C + E \underset{k_{-1}}{\overset{k_1}{\rightleftharpoons}} CE \overset{k_2}{\rightarrow} I_2 \overset{k_3}{\rightarrow} P_2 + E \qquad (2.6)$$

Where (2.5) and (2.6) describe the conversion of nitrocefin (N) and clavulanic acid (C), respectively. E is the enzyme, NE and CE are the non-covalent complexes and I_i and P_i represent the covalent intermediates and the products, respectively. An example script is provided as Supplementary material. Equation (2.6) is equivalent to the conversion model, discussed in the Results section (2.2).

Inhibition recovery

All samples for inhibition recovery experiments were thermostated at 298 K, at the concentrations indicated in Table 2.3. Activity measurements were performed by dilution in buffer without inhibitor to a final concentration of 2 nM BlaC with 100 µM nitrocefin. The time between initial dilution and measurement was kept <5 minutes and the reported time is that of the measurement. Separate incubations were performed to test the stability of BlaC without clavulanic acid, as well as clavulanic acid without BlaC.

Mass spectrometry

Samples for whole-protein mass spectrometry were flash-frozen in liquid nitrogen and stored at 193 K. Upon thawing, they were transferred to 10 mM ammonium acetate buffer pH 6.8 using Micro Bio-Spin® Chromatography Columns (Bio-Rad), loaded on a C4 polymeric reversed phase UPLC column and then analyzed using either an LTQ-Orbitrap mass spectrometer (ThermoScientific) or a Synapt G2-Si mass spectrometer (Waters), 10-25 minutes after thawing. Data were deconvoluted for charge using Thermo Xcalibur.

Nuclear Magnetic Resonance spectroscopy experiments

Samples for backbone assignment contained 0.75 mM [^{15}N,^{13}C,^{2}H] BlaC in 20 mM MES pH 6.0 with 1 mM DTT and 6% D_2O (NMR buffer) at 298 K. A set of standard HNCA, HNCACB, HNcoCACB, HNCO and HNcaCO experiments was recorded on a Bruker AVIII HD 850 MHz spectrometer equipped with a TCI cryoprobe for backbone assignment. All other NMR spectra, unless stated otherwise, were recorded on *ca.* 0.35 mM [^{15}N] BlaC samples in the same buffer at 298 K, on the same spectrometer. Data were processed with Topspin 3.2 (Bruker Biospin, Leiderdorp) and analyzed using CCPNmr Analysis.[143]

NMR titrations were performed by addition of an increasing volume of 0.9 M sodium phosphate or sodium chloride stock in NMR buffer to the sample, decreasing protein concentration from 0.35 to 0.25 mM during the titration. Non-linear regression fitting with a shared association constant (K_A) and individual maximal chemical shift perturbations (CSP) values (CSP_{max}) in Origin 9.1 was used to fit the CSP data of selected residues to Equation (2.7), in which R is the ratio of phosphate concentration over enzyme concentration, C_{stock} is the concentration of the phosphate stock solution used for titrating

and E_i is the initial concentration of enzyme in the sample. The phosphate titration was performed in duplicate. As the inter-experimental variation between samples was found to be larger than the intra-experimental variation between reporter peaks, data from the two experiments were fitted separately. Reported are the average and standard deviation of the two fits.

$$CSP = 0.5\, CSP_{max}\left(A - \sqrt{A^2 - 4R}\right)$$
$$A = 1 + R + \frac{C_{stock} + E_i\, R}{C_{stock}\, E_i\, K_A} \qquad (2.7)$$

Samples for NMR visualization of BlaC recovery from clavulanic acid inhibition contained 0.3 mM [^{15}N] BlaC and 1.5 mM clavulanic acid in 100 mM MES or sodium phosphate buffer, pH 6.4, with 1 mM DTT and 6% D_2O, at 298 K. Activity measurements as described above were performed at various time points to check the relation between spectra and functional states. Separate incubations were performed as controls on the stability of BlaC without clavulanic acid, as well as clavulanic acid without BlaC.

Supplementary material

Supplementary Tables

Table S2.1. Nitrocefin hydrolysis by BlaC with and without His-tag. [a]

BlaC	k_{cat} (s^{-1})	K_m (μM)	k_{cat}/K_m ($\cdot 10^5$ $M^{-1}s^{-1}$)
His-tagged	81 ± 7	73 ± 3	11.1 ± 0.4
Not tagged	77 ± 1	80 ± 1	9.5 ± 0.1

[a] Buffer was 100 mM MES, pH 6.4. Errors represent the standard deviation over duplicate measurements.

Table S2.2. Simulation parameters of BlaC inhibition by clavulanic acid. [a]

	K_D [b] (μM)	k_a ($\mu M^{-1}s^{-1}$)	k_b (s^{-1})	k_c (s^{-1})	K_I (μM)	k_1 ($\mu M^{-1}s^{-1}$)	k_2 (s^{-1})	k_3 (10^{-4} s^{-1})
MES 100 mM, pH 6.4	170	1.05	3000	148	20	1	0.045	0.25
NaP_i, 100 mM, pH 6.4	220	1.05	2500	103	20	1	0.045	18

[a] The parameters used for the simulations shown in Figure S2.5 are listed. The model is described in equations (2.5) and (2.6). Note that some parameters are correlated and the values should be considered as indicative. The large difference in k_3 under different buffer conditions is, however, very significant. The concentrations of BlaC and nitrocefin were 2 nM and 125 μM, respectively.
[b] $K_D = k_{-a}/k_a$

Table S2.3. M9 medium constituents per liter, in MilliQ water.

KH_2PO_4	13.0 g
K_2HPO_4	10.0 g
Na_2HPO_4	9.0 g
Na_2SO_4	2.4 g
$^{15}NH_4Cl$	0.3 g
Glucose	4.0 g
thiamine	30 mg
$MgCl_2$	2 g
Biotin	1 mg
Choline chloride	1 mg
Folic acid	1 mg
Niacinamide	1 mg
D-pantothenate	1 mg
Pyridoxal	1 mg
Riboflavin	0.1 mg
$FeSO_4$ (7 H_2O)	10 mg
$CaCl_2$ (2 H_2O)	60 mg
$MnCl_2$ (4 H_2O)	12 mg
$CoCl_2$ (6 H_2O)	8 mg
$ZnSO_4$ (7 H_2O)	7 mg
$CuCl_2$ (2 H_2O)	3 mg
H_3BO_3	0.2 mg
EDTA	50 mg

Supplementary figures

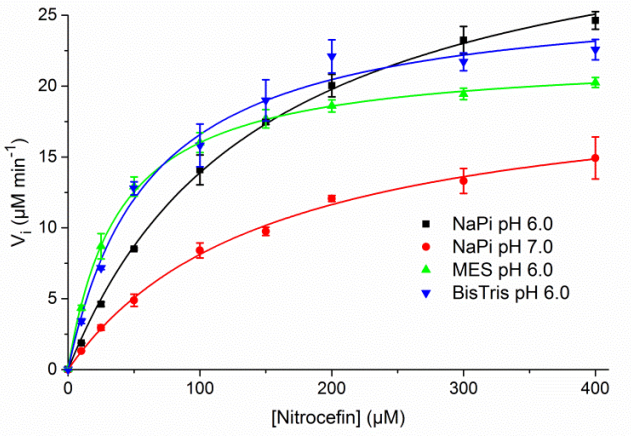

Figure S2.1. Michaelis-Menten curves for the hydrolysis of nitrocefin by 5.4 nM BlaC in various buffers. Error bars represent standard deviation of triplicate measurements.

```
1           11          21          31          41          51
MDLADRFAEL ERRYDARLGV YVPATGTTAA IEYRADERFA FCSTFKAPLV AAVLHQNPLT
  30          40          50          60          70          80    88

61          71          81          91          101         111
HLDKLITYTS DDIRSISPVA QQHVQTGMTI GQLCDAAIRY SDGTAANLLL ADLGGPGGGT
90          100         110         120         130         140  145 145

121         131         141         151         161         171
AAFTGYLRSL GDTVSRLDAE EPELNRDPPG DERDTTTPHA IALVLQQLVL GNALPPDKRA
    150         160         170         180         190         200

181         191         201         211         221         231
LLTDWMARNT TGAKRIRAGF PADWKVIDKT GTGDYGRAND IAVVWSPTGV PYVVAVMSDR
    210         220         230         240         250         260    267

241         251         261         271
AGGGYDAEPR EALLAEAATC VAGVLALEHH HHHH
    270         280         290
```

Figure S2.2. Amino acid sequence of the BlaC protein used in this chapter. The upper numbering corresponds to the actual sequence, the lower to the Ambler notation.[51] Residues 2-266 (upper numbering) are residues 43-307 of BlaC Uniprot sequence P9WKD3-1. The His-tag residues are highlighted in grey.

```
-26        -16        -6     0
 MGSSHHHHHH SSGLVPRGSH MENLYFQ


 1          11         21         31         41         51
 GDLADRFAEL ERRYDARLGV YVPATGTTAA IEYRADERFA FCSTFKAPLV AAVLHQNPLT
   30         40         50         60         70         80    88

 61         71         81         91         101        111
 HLDKLITYTS DDIRSISPVA QQHVQTGMTI GQLCDAAIRY SDGTAANLLL ADLGGPGGGT
 90         100        110        120        130        140  145 145

 121        131        141        151        161        171
 AAFTGYLRSL GDTVSRLDAE EPELNRDPPG DERDTTTPHA IALVLQQLVL GNALPPDKRA
     150        160        170        180        190        200

 181        191        201        211        221        231
 LLTDWMARNT TGAKRIRAGF PADWKVIDKT GTGDYGRAND IAVVWSPTGV PYVVAVMSDR
     210        220        230        240        250        260    267

 241        251        261
 AGGGYDAEPR EALLAEAATC VAGVLA
     270        280        290
```

Figure S2.3. Amino acid sequence of the BlaC protein with cleavable His-tag. The upper numbering corresponds to the sequence of the protein after cleavage, the lower to the Ambler notation.[S1] Residues 2-266 (upper numbering) are residues 43-307 of BlaC Uniprot sequence P9WKD3-1. The residues of the TEV-cleavable His-tag are highlighted in grey. The sequence after cleavage with TEV protease (residues 1-266, no highlight) is the same as that shown in Figure S2.2, except that the N-terminal Met in that sequence is replaced by Gly and the eight residues constituting the C-terminal His-tag are lacking.

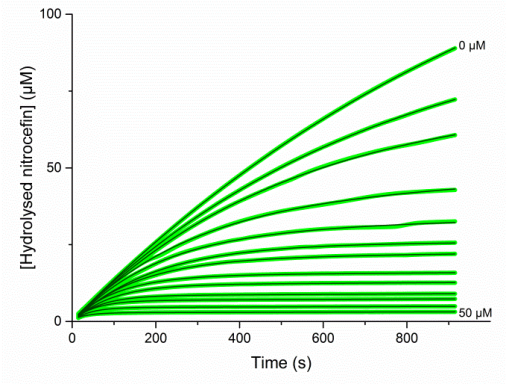

Figure S2.4. Inhibition curves of BlaC nitrocefin hydrolysis with increasing concentrations of clavulanic acid in 100 mM MES buffer pH6.4. Green lines represent experimental data, black lines are fits using equation 1.

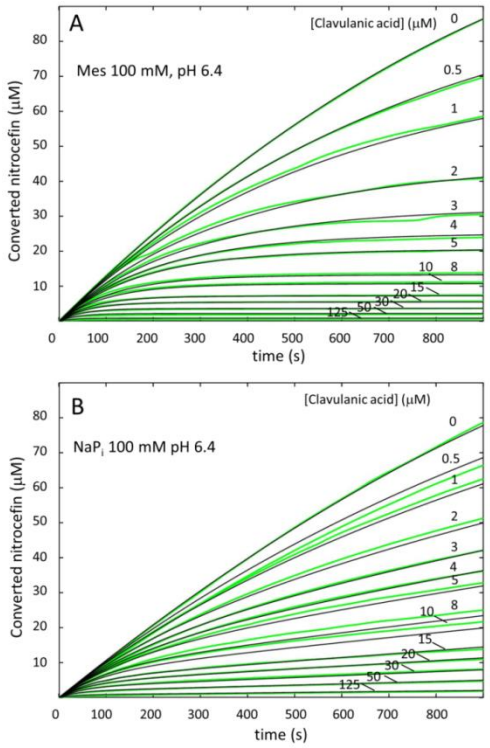

Figure S2.5. Inhibition of BlaC nitrocefin hydrolysis by clavulanic acid, in MES buffer (A) and phosphate buffer (B). The experimental curves (green) were simulated using GNU Octave software (black) and the models described in equations (2.5) and (2.6). [Nitrocefin], 125 μM; [BlaC], 2 nM; temperature, 298 K. The concentrations of clavulanic acid and the buffer conditions are indicated. Note the difference in the slopes of the curves at the end of the experiments. The larger slopes in NaP$_i$ buffer reflect the larger hydrolysis of BlaC-clavulanic acid intermediate (rate constant k_3).

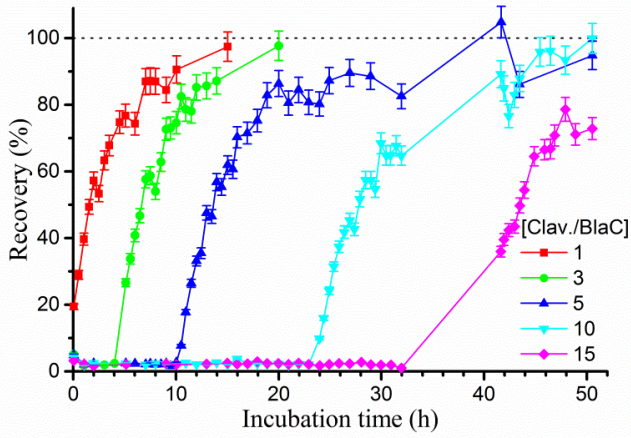

Figure S2.6. BlaC recovery from clavulanic acid inhibition with varying inhibitor / enzyme ratios. BlaC (100 µM) was incubated with 0.1, 0.3, 0.5, 1 and 1.5 mM clavulanic acid, respectively. Samples were taken at various time points, diluted to 2.0 nM BlaC and tested for hydrolase activity using 100 µM nitrocefin. Between 32 and 41.5 h, no measurements were performed due to a technical failure. The error bars are relative to the activity and represent the standard deviation in the 100% activity control measurements.

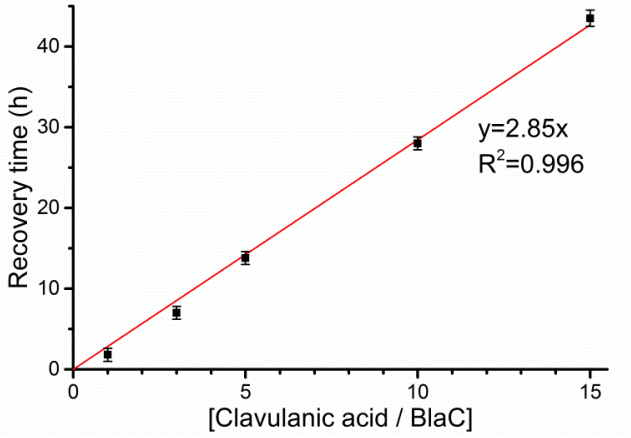

Figure S2.7. Relation between recovery time and molar ratio of enzyme and inhibitor. Recovery times (black squares) are the incubation times required to reach 50% activity, as estimated from Figure S2.6. Error bars represent the estimated error in reading recovery times from single curves. The text inset describes the linear fit through the origin, consistent with a first order reaction (red line). The slope represents the turn-over rate in h^{-1}.

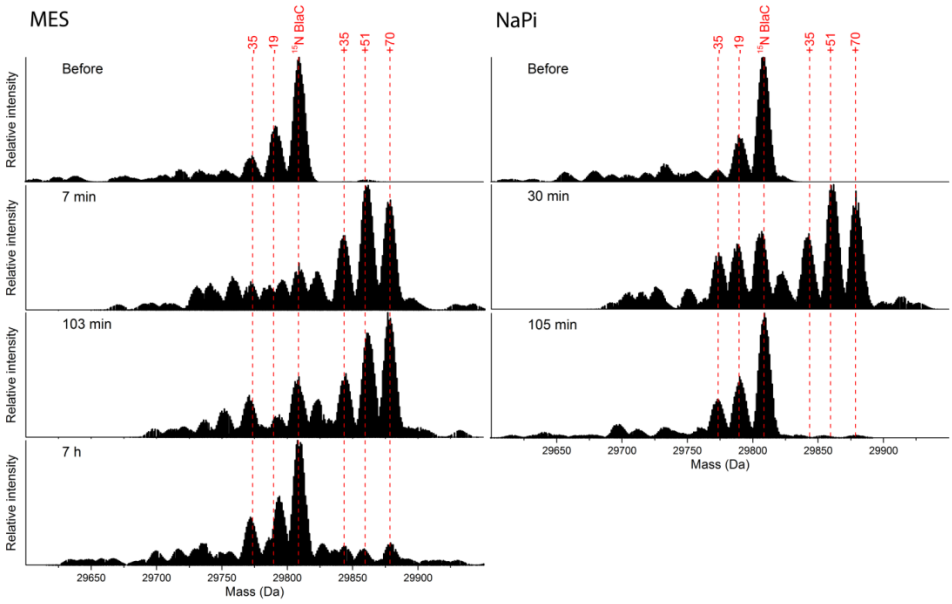

Figure S2.8. Charge-deconvoluted ThermoScientific Orbitrap mass spectra of BlaC before and during incubation with 1.5 mM clavulanic acid (protein: clavulanic acid ratio 1:5) in 100 mM MES (left) or NaPi (right) buffer, pH 6.4. Upon inhibition with clavulanic acid, the main species contain covalently bound adducts. After prolonged incubation, the enzyme returns to its free form in either buffer, but with different rates. For this experiment, ^{15}N labelled BlaC was used. This sample was also used in the NMR experiment. Each spectrum was normalised to the highest signal intensity.

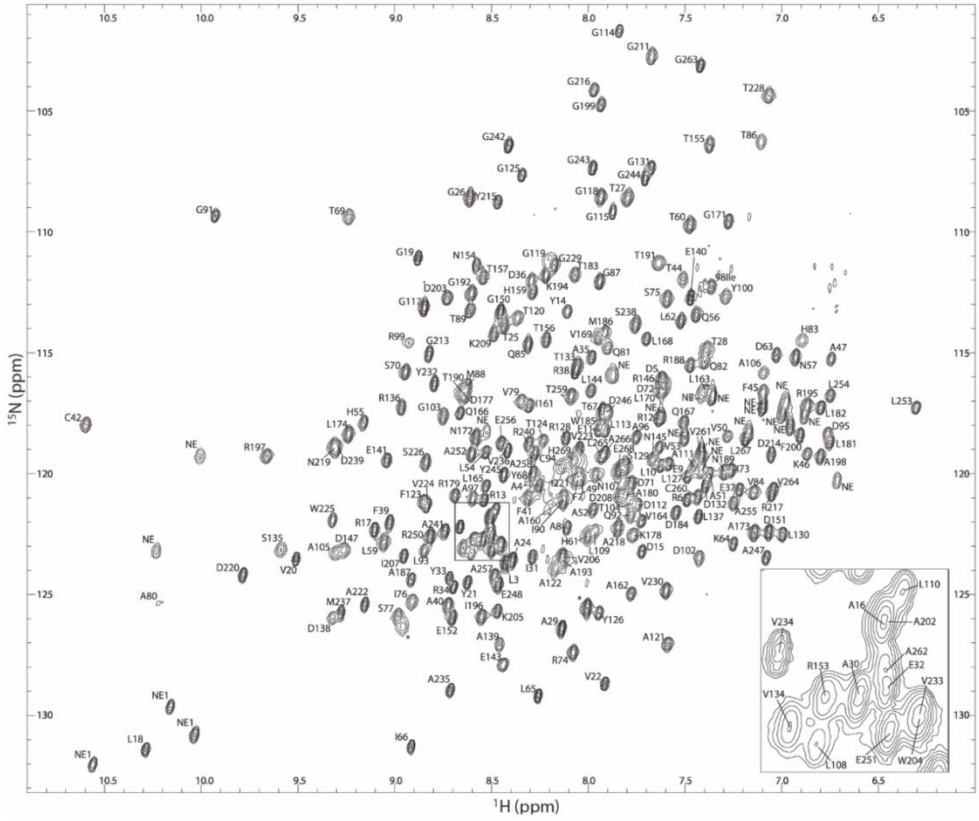

Figure S2.9. TROSY-HSQC spectrum of BlaC with residue assignments. 'NE' labels indicate arginine amide ε signals, 'NE1' labels indicate tryptophan amide ε1 signals. Numbering refers to the protein as it was measured, conversion to the Ambler numbering scheme can be found in Figure S2.2. The assignment can be accessed under Biological Magnetic Resonance Bank ID 27067.

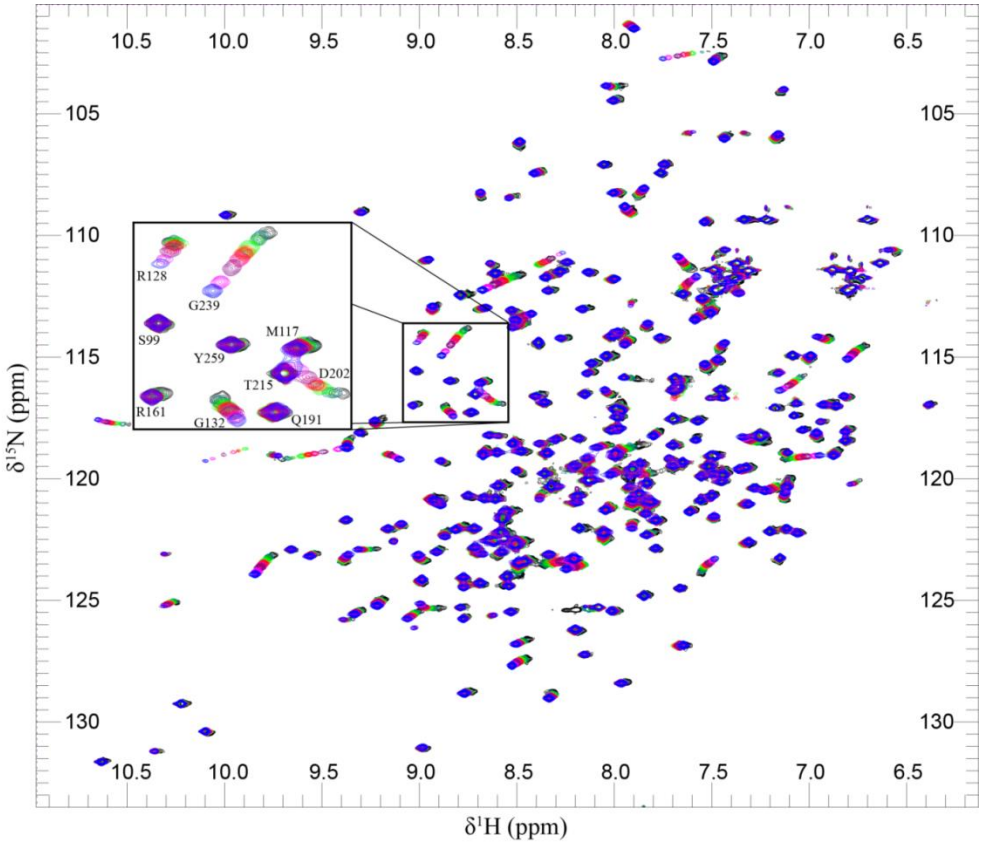

Figure S2.10. Overlay of ^{1}H-^{15}N HSQC spectra of BlaC upon titration with phosphate. The sample contained 350 µM BlaC, 20 mM MES buffer, pH 6.2, 1 mM DTT, 6% D_2O, without (blue peaks) and with 5 mM (magenta), 10 mM (purple), 15 mM (pink), 20 mM (red), 30 mM (orange), 50 mM (lime), 100 mM (green), 150 mM (teal) or 250 mM (black) of sodium phosphate, respectively. Selected residue numbers are shown.

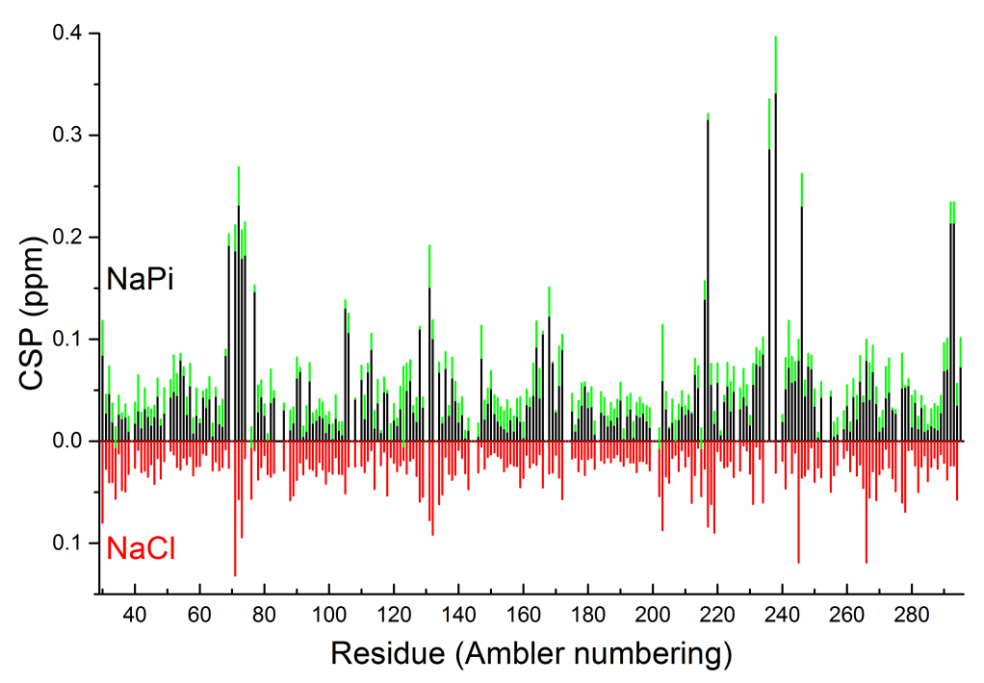

Figure S2.11. Absolute amide CSP upon titration from 0 – 250 mM with sodium phosphate (NaPi) or chloride (NaCl). Green error bars represent standard deviation over duplicate measurements.

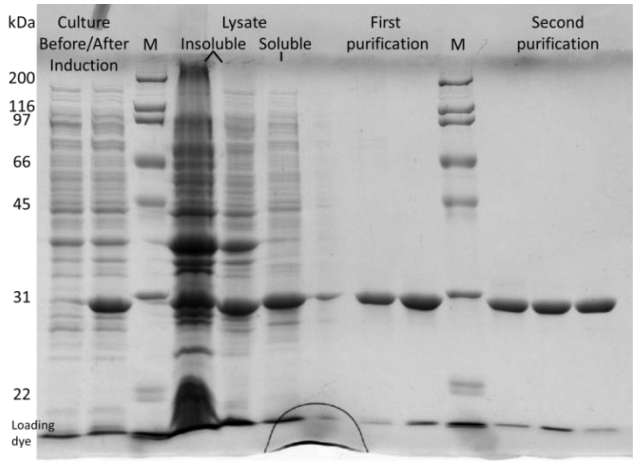

Figure S2.12. SDS-PAGE illustrating the production and purification process of BlaC (29 kDa). Minor impurities present after the first (Nickel column) purification are no longer visible after the second (gel filtration column) purification. This gel shows a representative protein batch. 'M' indicates a protein ladder, with band sizes shown on the left.

Octave script for simulation of inhibition curves

```
#! /usr/bin/octave -qf
# S(1) + E(2) k2<Ki>k1 SE(3) >k3 PSE(4) >k4 PS(5) + E(2)
# I(6) + E(2) k6<K2i>k5 IE(7) >k7 PIE(8) >k8 PI(9) + E(2)

# Load data and adjust
delay = 15;#deadtime
ext = 0.0173;              #extinction coeff of product in uM-1cm-1
data = load ("WE_BlaC_CLA_Phosphate_inhibition_data.txt");
time = data(:,1)-delay;
#abs = data(:,2:end)/ext; #convert abs to conc in uM
abs = data(:,2:end); #data already in uM
conc = load ("WE_BlaC_CLA_Phos_CLAconcen.txt"); #conc of clavulanate in each exp
m1 = rows(abs);
m2 = abs(1,:);

for i = 1:m1
 abs(i,:) = abs(i,:)-m2;
endfor

num1 = numel(conc);
num2 = numel(time);
res = zeros(num2,num1);
sq = zeros(num1,2);
sq(:,1)=conc';

for i = 1:num1
#for i = 1:1

con = conc(i);

# Define rates and differential equations
function xdot = f (x,t)
  Ki = 220;
  k1 = 1.05;
  k2 = Ki*k1;
  k3 = 2500;
  k4 = 103;
  K2i = 20;
  k5 = 1;
  k6 = K2i*k5;
  k7 = 0.045;
  k8 = 0.0018;
  xdot = zeros (9,1);
  xdot(1) = -k1*x(1)*x(2)+k2*x(3);
  xdot(2) = -k1*x(1)*x(2)+k2*x(3)+k4*x(4)-k5*x(6)*x(2)+k6*x(7)+ k8*x(8);
  xdot(3) = k1*x(1)*x(2)-(k2+k3)*x(3);
  xdot(4) = k3*x(3)-k4*x(4);
  xdot(5) = k4*x(4);
  xdot(6) = -k5*x(6)*x(2)+k6*x(7);
  xdot(7) = k5*x(6)*x(2)-(k6+k7)*x(7);
  xdot(8) = k7*x(7)-k8*x(8);
  xdot(9) = k8*x(8);

endfunction;
x0 = [125; 0.002; 0; 0; 0; con; 0; 0; 0];
#t = logspace(-3,8,10000);          #adjust to see entire range
```

```
y = lsode ("f", x0, time);
res(:,i) = y(:,5);
sq(i,2) = sum((abs(:,i)-res(:,i)).^2);

endfor

sqsum = sum(sq(:,2));
sqsum

# Plot the results

## Log plot of all concentrations
#plot (log10(t),log10(y));
#limits = axis([-3,8,-4,2]);
#xlabel ("log(10) time (s)");
#ylabel ("log(10) concentration (uM)");
#legend ("S", "E", "SE", "PSE", "PS", "I", "IE", "PIE", "PI", "location", "west");

#pause();

# Normal plot of data and predicted product curve
figure('Position',[100,350,1000,850]);
plot (time, abs, "-k", time, res,"-r");
limits = axis([1, 900, 0.1, 90]);
xlabel ("time (s)");
ylabel ("concentration (uM)");

print -djpg WE_BlaC_CLA_Phosphate_inhibition_data.jpg;
#save simul02.txt sqsum sq
pause();
```